Human Anti-CXCR4 Antibodies Undergo V_H Replacement, Exhibit Functional V-Region Sulfation, and Define CXCR4 Antigenic Heterogeneity[1]

Chen Xu,*† Jianhua Sui,*† Hong Tao,* Quan Zhu,*† and Wayne A. Marasco[2]*†

The chemokine receptor CXCR4 and its ligand stromal-derived factor-1 (SDF-1/CXCL12) are essential for many biological processes and various pathological conditions. However, the relationship between CXCR4 antigenic structure and SDF-1-mediated biological responses is poorly understood. In this report, a panel of human anti-CXCR4 Abs were isolated and used to explore CXCR4 antigenic heterogeneity and function. Multiple fixed CXCR4 antigenic isoforms were detected on the surface of hemopoietic cells. Epitope mapping studies demonstrated the complex nature of the surface-exposed CXCR4 epitopes. Ab-mediated inhibition of chemotaxis correlated strongly with binding affinity, epitope recognition, as well as the level of CXCR4 isoform expression. In addition, detailed genetic analyses of these Abs showed evidence of V_H replacement. Importantly, structural and biochemical studies demonstrated tyrosine sulfation in novel regions of the V genes that contributed bidirectionally to the binding activity of the Abs. These data provide the first evidence that functional tyrosine sulfation occurs in self-reactive Abs and suggest a potential new mechanism that may contribute to the pathogenesis of Ab-mediated autoimmune disease. These Abs also provide valuable tools to explore the selective in vivo targeting of CXCR4 isoforms that may be preferentially expressed in certain disease states and involved in steady-state CXCR4-SDF-1 homeostasis. *The Journal of Immunology,* **2007, 179: 2408–2418.**

The chemokine receptor CXCR4 is a seven-transmembrane G protein-coupled receptor for stromal cell-derived factor (SDF-1,[3] also named CXCL12) and is expressed in a wide range of different cell types and tissues. Both CXCR4 and SDF-1 are critically important in embryogenesis; gene knockouts of either are fatal as a result of disruption in hemopoietic, angiogenic, and neural development (1). In the adult, CXCR4-SDF-1 interactions are centrally involved in hemopoiesis, leukocyte trafficking, immune responsiveness, and angiogenesis (2–5). Modulation of CXCR4 expression has also been implicated in a variety of pathological conditions including inflammation and cancer where CXCR4-mediated activation of prosurvival pathways such as PI3K and Akt has been implicated as a mechanism by which cancer cells can evade host immunity and increase their metastatic properties (6–10). CXCR4 expression has been found in 23 different cancerous tissues (11–13) and in the case of solid tumors, hypoxia-inducible factor-1, a central mediator of tissue hypoxia, likely mediates the enhanced SDF-1 and CXCR4 expression (9). In addition, CXCR4 has been proposed to play a major role in tumor regrowth from cancer stem cells (14). In combination with CD4, CXCR4 also provides a coreceptor function for HIV-1 by forming a binding complex with HIV-1 envelope glycoprotein (gp120), which facilitates cell fusion and viral entry by CXCR4 using strains of HIV-1 (15, 16).

Cell surface CXCR4 reacts multifunctionally to SDF-1 exposure and promotes a variety of proliferative, differentiative, survival, morphological, chemotactic, and adhesive cell responses (1). This raises questions of whether CXCR4 is expressed as functionally different isoforms between cell types or even on the surface of individual cells and how CXCR4-SDF-1 interactions might be mediated or controlled. These questions are particularly pertinent considering CXCR4's constitutive expression by most body tissues and the keen interest in investigating CXCR4 as a therapeutic target (1, 17). Indeed, numerous posttranslational modifications of CXCR4 have been reported including *N*-glycosylation (18–20), disulfide formation (21), tyrosine sulfation (22, 23), serine chondroitin sulfation (22), oligomerization (24, 25), and proteolysis (26–28). Several studies have documented structural and functional heterogeneity in CXCR4 as well (19, 22).

Antigenically distinct conformations of CXCR4 have been previously reported (29, 30). The murine mAbs used in these studies mainly mapped to extracellular loop (ECL) 2. Although both studies showed that different antigenic isoforms of CXCR4 were expressed on different cells, they differed in their findings with regard to the number of antigenic isoforms and their distribution among different immune cells. The findings nevertheless raise the possibility that identifying a particular CXCR4 antigenic signature of a cell may provide important information regarding CXCR4 structure and functional responses to SDF-1 and HIV-1.

The purpose of this study was to isolate human anti-CXCR4 Abs for studies of receptor antigenic heterogeneity and function. A panel of human Abs was identified from a large, nonimmune human Ab phage library. Ab-binding studies provided strong evidence of CXCR4 antigenic heterogeneity on the cell lines that were examined. In addition, the Abs exhibited unique structural and biochemical features. The genetic studies revealed evidence of

*Department of Cancer Immunology and AIDS, Dana-Farber Cancer Institute and †Department of Medicine, Harvard Medical School, Boston, MA 02115

Received for publication February 13, 2007. Accepted for publication June 11, 2007.

The costs of publication of this article were defrayed in part by the payment of page charges. This article must therefore be hereby marked *advertisement* in accordance with 18 U.S.C. Section 1734 solely to indicate this fact.

[1] This work was supported by National Institutes of Health Grants AI060456 and AI52829 (to W.A.M.), AI58804 (to Q.Z.), as well as a Susan Komen Postdoctoral Fellowship PDF0202044 (to J.S.) from the Susan Komen Breast Cancer Foundation.

[2] Address correspondence and reprint requests to Dr. Wayne A. Marasco, Department of Cancer Immunology and AIDS, Dana-Farber Cancer Institute, Harvard Medical School, 44 Binney Street, Boston, MA 02115. E-mail address: wayne_marasco@dfci.harvard.edu

[3] Abbreviations used in this paper: SDF, stromal-derived factor; ECL, extracellular loop; PMPL, paramagnetic proteoliposome; GMFI, geometric mean fluorescence intensity; FW, framework domain; TM, transmembrane domain; MD, multidomain; Nt, N-terminal; VH/VL, variable region of Ig H chain or L chain.

V_H replacement in the formation of the rearranged V_H genes and the protein studies showed sulfation of tyrosine residues within V regions that have not been previously described (31, 32). Importantly, for several Abs, the V-region tyrosine sulfation was functional and contributed bidirectionally to CXCR4-binding affinity depending on the individual Ab. These studies demonstrate for the first time that tyrosine sulfation contributes to the activity of self-reactive Abs and suggest possible involvement of tyrosine-sulfated Abs in the pathogenesis of autoimmune disease (33). Furthermore, because these Abs recognize different CXCR4 isoforms, they should prove valuable for studies that examine modulation of the CXCR4-SDF-1 axis in health and disease and may be useful for diagnostic and/or therapeutic applications.

Materials and Methods

Cell culture

The canine thymus-derived cell line Cf2Th and human embryonic kidney cell line 293T were grown in DMEM (Invitrogen Life Technologies) supplemented with 10% (v/v) heat-inactivated FCS, 100 IU/ml penicillin, and 100 μg/ml streptomycin (total DMEM) at 37°C with 5% CO_2. Stably transfected cell line Cf2ThCXCR4C9 (Cf2X4C9), which expresses codon-optimized CXCR4 (synCXCR4) containing a C9 tag (TETSQVAPA) at its C terminus (34), was grown in the total DMEM containing 500 μg/ml G418. Cf2ThCD4CXCR4 (X4T4) cells were grown in total DMEM plus 500 μg/ml G418 and 200 μg/ml hygromycin B. Human T lymphocytic leukemia cell line Jurkat was grown in RPMI 1640 containing 10% (v/v) heat-inactivated FCS.

Abs and reagents

The sources for Abs and reagents are: both purified and PE-conjugated anti-CCR5 (2D7) and -CXCR4 (12G5) mouse mAbs and IgG2a isotype control (BD Pharmingen); the 1D4 mAb reacting with a C9 peptide (University of British Columbia, Vancouver, Canada); FITC-goat anti-human IgG and FITC-goat anti-mouse IgG (Sigma-Aldrich); and purified and HRP-labeled mouse IgG against M13 (Amersham Biosciences). Other reagents included *Escherichia coli* TG1 and helper phage VCS M13 (Stratagene), G418 (Gellgro), and tetramethylbenzidine substrate and stop solution (KPL).

Preparation and characterization of CXCR4-containing paramagnetic proteoliposomes (CXCR4-PMPLs)

The method used to prepare CXCR4-PMPLs was described previously (34, 35). In brief, 1×10^8 Cf2X4C9 cells were lysed with 1% CHAPSO and then incubated with 0.5×10^9 M-280 Dynal beads (Dynal Biotech) coated with 1D4 mAb. The protein-bound beads were washed six times and resuspended in buffer containing 100 mM $(NH_4)_2SO_4$, 20 mM Tris (pH 7.5), and 1 mg/ml lipid mixture consisted of POPC/POPE/DOPA (Avanti Polar Lipids) and then dialyzed to remove detergent and allow the formation of proteoliposomes.

To evaluate the CXCR4-PMPL protein content, Cf2X4C9 cells were radiolabeled with [^{35}S]methionine/cysteine (PerkinElmer Life Sciences) and used for formation of CXCR4-PMPLs. A total of 3×10^7 proteoliposomes were treated with 2× SDS sample buffer and the eluted sample was separated by SDS-PAGE followed by autoradiography analysis (KODAK BioMax Film and Fisher Biotech autoradiography cassette).

The native conformation of CXCR4 captured on PMPLs was detected by staining with the CXCR4-specific conformation-dependent mAb 12G5 and the exclusive ligand of CXCR4 (SDF-1α). A total of 1×10^6 CXCR4-PMPLs were incubated with 20 μl of PE-coupled 12G5 mAb for 45 min at 4°C. The isotype-matched control Ab and CCR5-specific mAb 2D7 were used as negative controls. PMPLs were washed in PBS/0.5% BSA/0.02% NaN3 and analyzed by flow cytometric analysis on a BD Biosciences FACScan apparatus with CellQuest software.

Selection of anti-CXCR4 single-chain Abs from nonimmune human scFv phage display library with PMPL panning

The Ab selection procedure including CXCR4-PMPL panning, cell-based ELISA screening, and confirmation by flow cytometric analysis as well as DNA sequencing were essentially following the procedure describe previously (35, 36). Cf2Th cells, CCR5-PMPLs, and CXCR4 PMPLs were preblocked in blocking buffer (2% BSA/2% nonfat milk/PBS) at 4°C for 30 min. A total of 5×10^{12} PFU phage library was incubated with 2×10^7 Cf2Th cell and 2×10^7 CCR5 PMPLs for three separate times to absorb the nonspecific clones. The 15 and 12 billion member human scFv-phage display (Mehta I/II) libraries (S. Mehta and W. A. Marasco, unpublished data), respectively, were pooled and then incubated with 5×10^7 CXCR4 PMPLs preblocked in 3 ml of 4% BSA/4% nonfat milk/PBS for 2 h at 4°C with gentle shaking. Unbound phages were removed by washing with 3 ml of PBS containing 0.1% Tween 20. Phage bound to CXCR4-PMPLs was eluted by addition of 1 ml of 100 mM triethylamine and incubation for 20 min at room temperature. The mixture was neutralized with an equal volume of 1 M Tris-HCl (pH 6.8). The PMPLs were pelleted and half of the supernatant was used for phage titration and infection of an exponentially growing culture of *E. coli* TG1 for next round of panning. Three rounds of PMPL-based panning were performed.

Cell-based ELISA with phage scFv Abs

Single colonies from the second and third rounds of panning were picked randomly and phage were rescued. Cell-based ELISA screening for individual phage scFv Ab clone was performed as follows: 2×10^5 X4T4 cells or Cf2Th cells were incubated with 70 μl of phage supernatant for 1 h at 4°C. The unbound phage Abs were removed by washing cells three times with washing buffer (4% FBS/PBS). One hundred microliters of HRP-conjugated mouse anti-M13 mAb solution (1/4000 diluted in blocking buffer) was added, followed by incubation at 4°C for 45 min to detect cell surface-bound phage. Absorbance at 450 nm (A_{450}) was recorded in an ELISA reader. Clones were scored positive by ELISA if the OD_{450} for X4T4 cells was >5-fold over parental Cf2Th cells.

Subcloning, expression, and purification of soluble anti-CXCR4 scFvFc Abs

For scFvFc expression in mammalian cells, scFv-coding DNA fragments from the pFarber phagemid were excised by *Sfi*I/*Not*I digestion and subcloned into an eukaryotic expression vector (pcDNA3.1-hinge-stuffer), where the anti-CXCR4 scFv is fused in frame with the human IgG1 hinge-CH2-CH3 domains to form scFvFc fusions. 293FT cells were transfected with anti-CXCR4 scFvFc expression plasmids by the CaPO4 method and allowed to express in 293 SFM II serum-free medium (Invitrogen Life Technologies) containing 4 mM L-glutamine and 4 mM sodium butyrate. The cell culture supernatant containing scFvFc proteins was collected twice every 48 h and the Fc-containing Abs were purified by protein A affinity chromatography.

Flow cytometric characterization of the anti-CXCR4 Ab-binding activity

The binding of anti-CXCR4 Abs was examined by an indirect immunofluorescence assay. A total of 5×10^5 Jurkat or stable X4T4 cells were incubated with each serially diluted scFvFc Ab for 45 min at 4°C followed by staining with FITC-goat anti-human IgG. Anti-CXCR4 mouse mAb 12G5 treatment followed by FITC-goat anti-mouse IgG staining was used as a positive control. Cells were washed in PBS containing 0.5% BSA and analyzed on FACScan apparatus. The EC_{50} (concentration of Ab that reaches half-maximal for percent cell binding and geometric mean fluorescence intensity (GMFI), respectively) were used as a measure of the relative binding affinity of each scFvFc to CXCR4-positive cells.

Inhibition of Jurkat cell chemotaxis induced by SDF-1α

A total of 2×10^5 Jurkat cells were incubated with 100 μl of chemotaxis buffer (0.1% BSA/RPMI 1640 medium) with or without indicated amounts of anti-CXCR4 scFvFc at 37°C for 30 min. Human CCR5-specific A8 scFvFc (S. Wei, C. Xu, J. Sui, Q. Zhu, and W. A. Marasco, unpublished data) and 12G5 mouse IgG were used as negative or positive control, respectively. Cell suspension was transferred to the upper well of a Corning Costar Transwell (6.5 mm diameter, 5.0 μm pore size) where the lower chamber contained 50 ng/ml human SDF-1α (concentration chosen after a complete dose-response curve was established for SDF-1α-induced chemotaxis of Jurkat cells) in 600 μl of chemotaxis buffer. After incubation for 4 h at 37°C in a 5% CO_2 incubator, cells migrated into lower wells (in duplicates) were collected and cell number was counted with Flow-Check Fluorosperes (BD Biotechnology) as markers on FACScan. Percentage of inhibition was calculated with the following formula: percent of inhibition = 100 × (1 − average cell number under treatment of Abs/average cell number without treatment).

Epitope mapping anti-CXCR4 scFvFc Abs

CXCR4/CXCR2 chimera and N11Q CXCR4 mutant studies. Chimeric receptors composed of human CXCR4 and CXCR2 were provided by

Dr. R. W. Doms (Department of Pathology and Laboratory Medicine, Department of Medicine, University of Pennsylvania, Philadelphia, PA) (37). 293T cells were transiently transfected with each chimeric CXCR4/CXCR2 receptor plasmid as well as synCXCR4 or CXCR2 plasmids. Upon 48 h of posttransfection, cells were harvested with 5 mM EDTA/PBS and the binding of each anti-CXCR4 scFvFc Abs was examined by an indirect immunofluorescence assay through FACScan. The binding activity was calculated with the following formula: percent = 100 × (GMFI of CXCR4 variants − GMFI of 293T cells)/(GMFI of wild-type CXCR4 − GMFI of 293T cells). In the studies comparing the scFvFc binding to stable Cf2 cells expressing CXCR4 wild type and N11Q mutant, the activity was normalized to 12G5 binding.

AMD3100 inhibition and 12G5 competition studies. (1) A total of 5×10^5 X4T4 cells were treated in PBS with or without 250 ng of AMD3100 (5 μg/ml × 50 μl) at 4°C for 30 min followed by addition of anti-CXCR4 scFvFcs or 12G5 mAb. After 45 min, unbound Abs were removed and FITC-labeled goat anti-human-IgG or FITC-labeled goat anti-mouse-IgG was used to detect the Abs bound to the cell surface through flow cytometric analysis. The binding intensity was calculated as the following formula: percentage = 100 × GMFI of cells treated with AMD3100/GMFI of cells without treatment. (2) A total of 2.5 μg of anti-CXCR4 scFvFc or unlabeled mAb 12G5 were incubated with 5×10^5 X4T4 cells at 4°C for 30 min before the addition of PE-conjugated 12G5. After another 45-min incubation at 4°C, cells were washed and flow cytometric analysis was performed to detect the PE-12G5 binding intensity on cell surface. The percentage of inhibition on 12G5 binding was calculated as: percent of inhibition = 100 × (1 − GMFI of sample preincubated with anti-CXCR4 scFvFc/GMFI of 12G5 samples without treatment).

Sulfation studies

The metabolic radioisotope labeling method to detect sulfated protein was essentially used as described before (23). For sulfation inhibition studies, 100 mM sodium chlorate was added to 293 SFM II medium 18 h after transfection. After another 48 h, the secreted Abs were purified from culture supernatant with protein A-Sepharose beads. Specific tyrosine mutations were introduced into scFvFc expression constructs with the QuickChange Multi Site-Directed Mutagenesis kit (Stratagene) according to manufacturer's instructions and final mutant constructs were confirmed by DNA sequence analysis. The primers used for site-directed tyrosine mutagenesis are: X20-DD-V_HCDR2, 5′-GCAAGATGGAAGTGAGAAAG ACGATGTGGACTCTGTGAAGGG-3′; X20-D-V_L framework domain (FW) 3, 5′-AGGCTGAAGATGAGGCTGACGATTTCTGTAATTCCCG GAG-3′; X33-DD-V_HCDR2: 5′-ACATGATGGAACTAAGAAAGATGA CGCAGACTCCGTGAAGGG-3′; X33-DD-V_LFW3: 5′-GGCTGAGGAT GAGGCTGATGATGACTGCCTGTCCTTTGACAG-3′.

Results

Construction and characterization of CXCR4-containing paramagnetic proteoliposomes

Cell lysates from [^{35}S]cysteine/[^{35}S]methionine metabolically labeled Cf2X4C9 cells were used to form CXCR4-PMPLs. CXCR4-PMPLs were pelleted, treated with reducing buffer, and the supernatant was subjected to SDS-PAGE analysis. As shown in Fig. 1*A*, while no band detected from PMPLs formed with parental Cf2Th cell lysates (*lane 2*), only one predominant band was observed by autoradiography with the expected molecular mass of mature CXCR4 (46 kDa) in PMPLs formed with Cf2X4C9 cell lysates (*lane 1*). As shown in Fig. 1*B*, in addition to CXCR4, two other protein bands were detected by silver staining which correspond to the 1D4 mAb H chain (50 kDa) and L chain (25 kDa). Other cellular proteins were present at only trace levels. The integrity of CXCR4 secondary structure in the PMPLs was also evaluated by binding of the conformationally sensitive anti-CXCR4 mAb 12G5 through flow cytometric analysis. As shown in Fig. 1*C*, PE-labeled 12G5 mAb bound to CXCR4-PMPLs efficiently whereas isotype-matched control IgG2a mAb did not bind as expected. The specificity of this binding was further demonstrated by failure of mAb 12G5 binding to control CCR5-containing PMPLs whereas mouse anti-CCR5 mAb 2D7, a conformation-dependent Ab against coreceptor CCR5, bound to CCR5-PMPLs but not to CXCR4-PMPLs. In addition to 12G5, the CXCR4 ligand SDF-1α also bound specifically to CXCR4-PMPLs. These results demonstrate that CXCR4 is selectively incorporated in its native state in highly enriched form into the PMPLs.

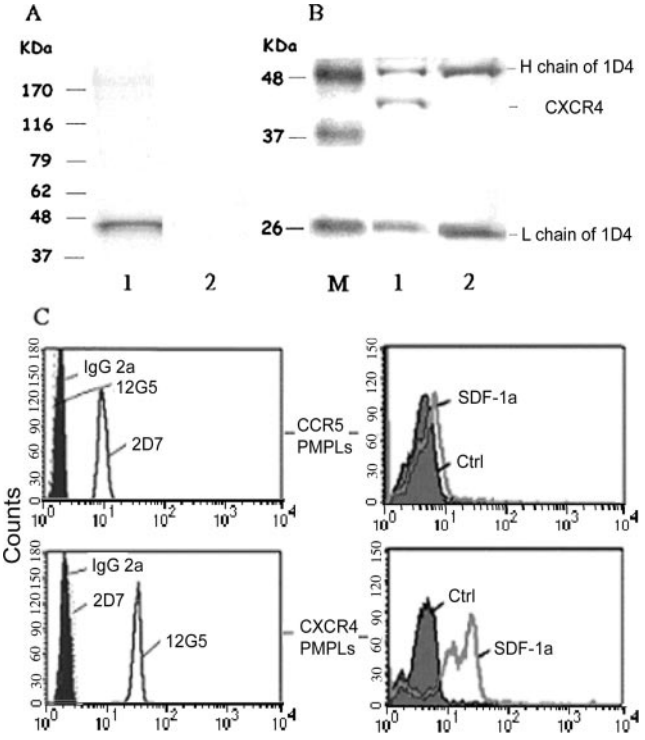

FIGURE 1. Characterization of CXCR4-PMPLs. *A*, PMPLs were made by incubating 1D4 mAb coated M280 Dynal beads with [^{35}S]methionine/cysteine-labeled Cf2X4C9 (*lane 1*) or Cf2Th (*lane 2*) cell lysates. Protein purity of the PMPLs was determined by SDS-PAGE followed by autoradiography analysis. *B*, A total of 5×10^7 CXCR4-PMPLs (*lane 1*) or M280 Dynal beads coated with 1D4 mAb only (*lane 2*) were treated with 2× SDS buffer for 1 h at 55°C followed by boiling for 5 min. The supernatant was used for SDS-PAGE analysis and proteins were visualized by silver staining. *C*, CXCR4-PMPLs (*lower*) were incubated with the CXCR4 conformational-dependent mAb 12G5-PE directly (*left*) or its natural ligand SDF-1-Fc fusion protein followed by FITC-anti-human IgG (*right*). CCR5-PMPLs (*upper*) with CCR5 specific mAb 2D7-PE as well as IgG2a-PE were used as negative controls.

Isolation of CXCR4-specific Abs from a phage display library

Twenty-three of 768 (2.99%) clones from the second round and 1 of 96 (1.04%) clones from third round of CXCR4-PMPL panning specifically bound to CXCR4-positive cells as detected by cell-based ELISA and confirmed by flow cytometric analysis with phage Abs (data not shown). DNA sequence analysis revealed six unique scFv clones (2N, X18, X19, X20, X33, and X48) from the second round of wild-type CXCR4-PMPLs panning and one clone (6R) from second round of N-terminal deleted (ΔN 2–25)-CXCR4-PMPL panning. Fig. 2 shows the complete V-region amino acid sequences of these clones. As can be seen, all clones show extensive diversity in the CDR regions. Three H chain families (V_H1, V_H3, and V_H6) are represented (Table I). V_H1–18 and V_H6–1 germline genes were each represented once; two V_H3 germline genes (V_H3–7 and V_H3–30) were used once (X20) and four times (2N, X19, X33, and X48), respectively. The H chain V-region genes can be roughly divided into two groups based on the length of CDR3 (Fig. 2). One group composed of three H chains (X18, X20, and X33) have longer CDR3 of 17–18 aa as compared with the average length of human CDR3s (13.1 aa). These same V_H chains also have a high content (3–4) of charged

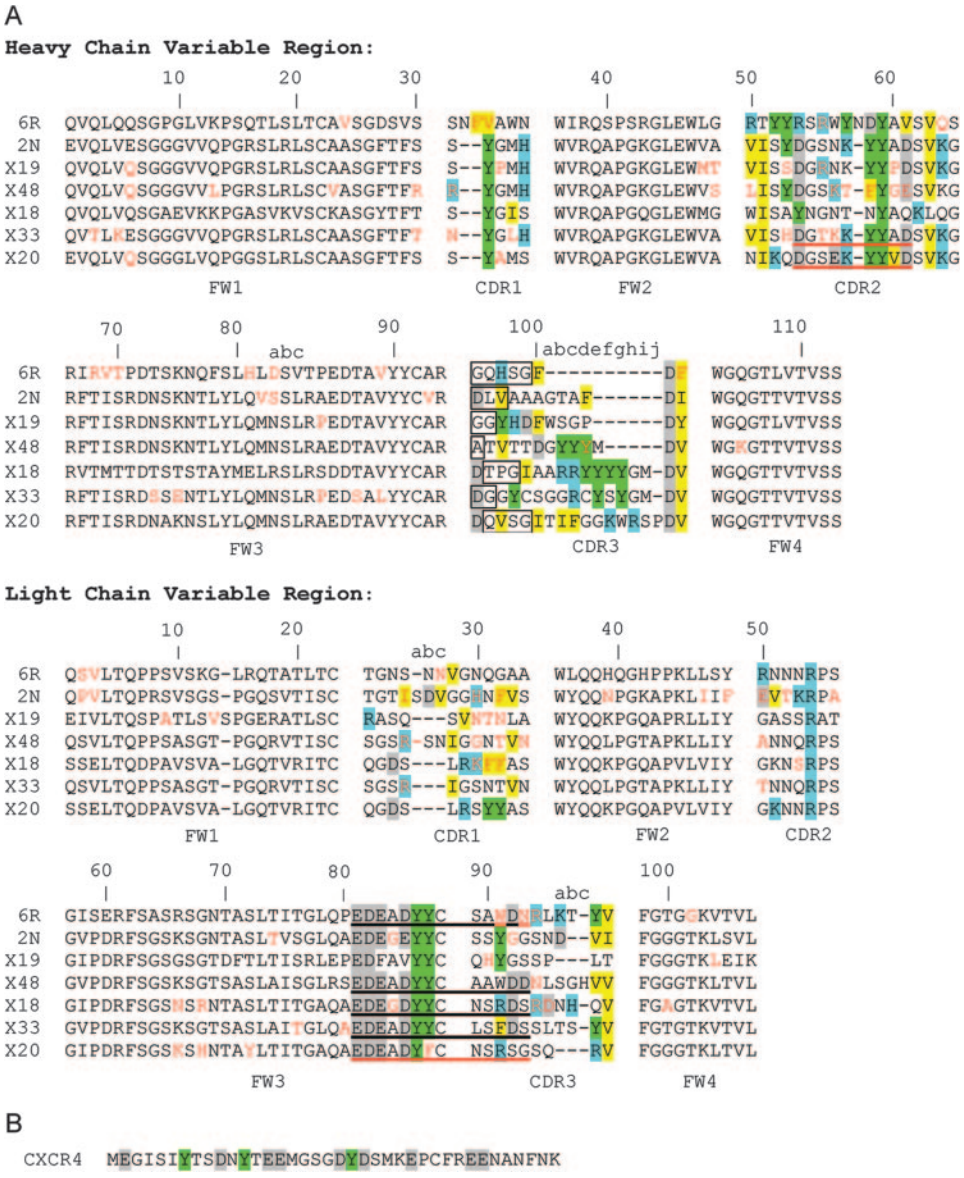

FIGURE 2. Amino acid sequences of anti-CXCR4 Ab variable regions (*A*) and N-terminal sequence of human CXCR4 (*B*). Kabat number system is shown above the Ab sequences. Tyrosine residues within all CDRs, FR L3, and Nt-CXCR4 are marked as green. The acidic residues (D and E) within CDR and Nt-CXCR4 are highlighted in gray. D and E residues of FR L3 that may involve in tyrosine sulfation are also marked. Basic (R, H, and K) and hydrophobic (I, F, and V) residues within CDR regions are labeled with blue and yellow, respectively. Sequences with somatic mutations are marked in red letters. The tyrosine sulfation sites predicted by "Sulfinator" software are underlined with black and visually verified tyrosine sulfation sites in X20 and X33 are underlined in red. The amino acids encoded by the V-D segment in H chain CDR3 are boxed.

amino acids. The second group contains four H chains with shorter CDR3s (6R, 2N, X19, and X48) ranging from 8 to 13 aa with two to three charged residues. Two of the V_H genes (*X18* and *X20*) with longer CDR3s contain a high content of hydrophobic (5 or 6) amino acids, while one V_H gene (*X48*) with a shorter CDR3 also contains 5 hydrophobic amino acids. X48 and X18 contained clusters of three and four tyrosines, respectively. Three L chain families (Vλ1, Vλ2, and Vκ3) including five germline genes (*V1-3*, *V1-20*, *V1-16*, *V2-13*, and *A27*) are represented (Table I). Interestingly, V_L CDR3 of two clones, 6R and X18, contained a high content of charged amino acids (3 and 5) (Fig. 2), respectively.

Evidence of V_H replacement

V_H replacement, the secondary rearrangement of an upstream V_H to a preformed $V_HD_HJ_H$ gene, has recently been shown to contribute to normal V_H repertoire development (38–41). Importantly,

Table I. *V and J germline gene usage in CXCR4-specific Abs*

Ab	H Chain			L Chain			V and J Mutations
	Family	V gene	J gene	Family	V gene	J gene	
2N	V_H3	*V_H3-30*	*J_H3*	Vλ1	*V1-3*	*J_L2*	17
6R	V_H6	*V_H6-1*	*J_H5*	Vλ1	*V1-20*	*J_L1*	19
X18	V_H1	*V_H1-18*	*J_H6*	Vλ2	*V2-13*	*J_L1*	10
X19	V_H3	*V_H3-30*	*J_H4*	Vκ3	*A27*	*JK4*	15
X20	V_H3	*V_H3-7*	*J_H6*	Vλ2	*V2-13*	*J_L3*	6
X33	V_H3	*V_H3-30*	*J_H6*	Vλ1	*V1-16*	*J_L1*	17
X48	V_H3	*V_H3-30*	*J_H6*	Vλ1	*V1-16/V1-17*[a]	*J_L2/J_{L3}*[a]	20

[a] These genes are equally homologous to both germline.

Table II. *Potential V_H replacement analysis of CXCR4-specific Abs*[a]

Ab	V_H Sequence	P	V-D	D_H Sequence	D_H Germline
2N	**TACTGTG***T*GAGAGA		TCTTG	TAGCAGCAGCTGGTAC	D6-13
6R	**TACTGTG**CAAG(AGA)		GG**GGCAGCACAG**CGG	TTTTGACT	D3-9
X18	**TACTGTG**CGAGAGA	T	ACCCCCGGA	ATAGCAGCTCG	D6-6
X19	**TACTGTG**CGAGAG		**GCGGC**	TATCACGATTTTTGGAGTGG	D3-3
X20	**TACTGTG**CGAGAGA	TC	AGGTTTCCG	GTATTACGATTTTTGGAG	D3-3
X33	**TACTGTG**CGAGAGA		CGGC	GGATATTGTAGTGGTGGTCGATGTTACTC	D2-15
X48	**TACTGTG**CAAGA(GA)		G	CTACAGTAACTAC	D4-4/D4-11[b]

[a] Nucleotide sequences were analyzed by IGBLAST and DNAPlot and the nomenclatures used in this table are from IGBLAST. The listed sequences are from the first nucleotide of the cryptic recombination signal sequence, which is in bold to the end of V_H segment. The nucleotides in parentheses are deleted from the V_H germline genes and the nucleotides italicized in 2N and X48 indicate C/T and G/A mutation, respectively. The pentamers in the V-D junction segment GGCAG, CACAG, and GCGGC match the 3′ end of V_H germline VH1-58, VH2-5, and VH1-58, respectively, and are shown in bold in the V-D column. The underlined region in V-D column may indicate a second V_H replacement.

[b] These genes are equally homologous to both germline.

the residual 3′ "footprint" sequences of replaced V_H genes have been shown to contribute charged amino acids in CDR3 (41). In addition, the frequency of charged amino acids within the V-D junction of V_H replacement products have been found at a higher frequency than those in the V-D junction of non-V_H replacement products or in the D-J junctions of normal Ig sequences (41). Table II shows the results of a V_H gene replacement analysis of the seven anti-CXCR4 Ab genes isolated. Two of the seven V_H regions (6R and X19) contain pentameric sequences corresponding to the 3′ end of known V_H genes. In the case of 6R, the analysis suggests that this V-D junction was formed by two sequential V_H replacement events, the first of which resulted in the placement of histidine in the CDR3. For X19, a single V_H replacement event appears to have occurred but it did not result in the gain of charged amino acids. This analysis did not provide evidence of V_H replacement for two other V_H CDR3s (2N and X33) that also had positive charges in the V-D junction sequences or for X18 and X20 where aspartic acid was encoded by "P" nucleotide additions.

Existence of fixed cell surface CXCR4 isoforms

The anti-CXCR4 scFvFcs were constructed, expressed, and purified. The binding activities of the bivalent proteins were further examined by flow cytometric analysis. The results demonstrated that all anti-CXCR4 scFvFcs could recognize CXCR4-positive cells, but not parental Cf2Th cells. In addition, there was no cross-reaction against several other seven-transmembrane domain receptors including CCR1, CCR2, CCR5, CCR8, CXCR1, GPR1, GPR15, STRL33, or APJ (data not shown). The relative affinity of each anti-CXCR4 scFvFc protein was analyzed by staining of the $CD4^+CXCR4^+$ Jurkat cells and stable X4T4 cells using serial dilutions of each Ab in saturation-binding studies. A commercial anti-CXCR4 mAb 12G5 was used as a positive control. The results were analyzed for both percentage of cells with positive staining and EC_{50} values (concentration of Ab which gave half-maximal GMFI). As shown in Fig. 3, *A* and *B*, for both cell types, all of the scFvFcs reached 100% positive binding at a relatively lower concentration comparing to that needed to obtain GMFI saturation (Fig. 3, *C* and *D*), respectively. The only exception was 6R scFvFc, which did not reach saturation on Jurkat cells or X4T4 cells, suggesting that 6R may not possess a high enough binding affinity to reach saturation. The concentration of Ab to reach half-maximal GMFI on Jurkat cells ranged 150-fold from 0.10 ± 0.01 μg/ml for X48 to 15.2 ± 1.40 μg/ml for X19 (Fig. 3*E*). Similarly, the EC_{50} for $GMFI_{MAX}$ to X4T4 cells varied over a 46-fold range from 0.48 ± 0.01 μg/ml for X18 to 22.0 ± 5.8 μg/ml for 6R. Importantly, the rank order of scFvFc binding was essentially identical for both of these cell lines. 12G5 mAb reached half-maximal binding at 0.91 ± 0.19 μg/ml for Jurkat cells which is mid-range compared with two previous reports, 1.9 ± 0.5 μg/ml (29) and 0.19 ± 0.05 μg/ml (30), respectively. Fig. 3*E* shows that the maximal $GMFI_{MAX}$ binding to Jurkat cells could be divided into three groups: X18 and X20 show the highest $GMFI_{MAX}$ while 2N, X19, X48, and 12G5 show intermediate binding, and X33 and 6R bind poorly to Jurkat cell. A similar result was seen for X4T4 cells. Interestingly, for neither of the cell lines did we observe a direct correlation between maximal binding (potency) and EC_{50} (efficacy). For example, X48 and 12G5 are two clones with the high relative affinities but only intermediate maximal binding on both cell lines (compare *A* and *B* to *C* and *D*). On the basis of the differences in maximal binding of the eight Abs to these two cell lines, the results support the existence of relatively fixed subpopulations of CXCR4 molecules on the cell surface that can be recognized by different Abs but the relative contributions of conformation and structure to antigenic heterogeneity of CXCR4 remains to be determined.

Inhibition of SDF-1 induced chemotaxis by anti-CXCR4 scFvFcs

The ability of anti-CXCR4 scFvFc to inhibit SDF-1α-induced chemotaxis of Jurkat cells was next investigated to determine whether CXCR4 antigenic heterogeneity, as evidenced by Ab recognition of different subpopulations of CXCR4 molecules, could differentially effect this receptor signaling. As shown in Fig. 4, X18 and X20 exhibited the most potent inhibition of SDF-1α chemotaxis where cell migration was reduced by ~60%, similar to mAb 12G5. In the presence of 10 μg of Abs, X48, the next strongest binding Ab, inhibited chemotaxis by ~40%, X33 by 30%, and 6R/X19 by ~20% while 2N did not inhibit chemotaxis at all.

Epitope mapping by flow cytometric analysis

CXCR4/CXCR2 chimera and CXCR4 N11Q mutant studies. To identify the Ab-recognition domains on CXCR4, the binding activity of each isolated scFvFc Ab to a panel of CXCR4/CXCR2 chimeric receptors (29) transiently expressed on 293T cells was examined by flow cytometric analysis. Comparable surface expression for each CXCR4/CXCR2 chimeric receptor was demonstrated by flow cytometry analysis using CXCR4-specific mAb 12G5 staining as a control which primarily recognizes an epitope located in ECL2 of human CXCR4 (29, 42, 43). As shown in Table III, none of the scFvFcs recognized wild-type CXCR2. Substitution of either the first 27 aa (2444) or replacement of the whole 38-aa N terminus (2444b) of CXCR4 by CXCR2 reduced staining intensity of most of the mAbs by >80%, with the only exception of X18 (34.5 and 32.2%, respectively). Five Abs, 2N, 6R, X20, X33, and X48, demonstrated strong binding to CXCR4-N-terminal (Nt) as evidenced by poor binding to all three chimeras (2444, 2444b, 2442) that lacked the CXCR4-Nt domain. When the ECL3 loop of

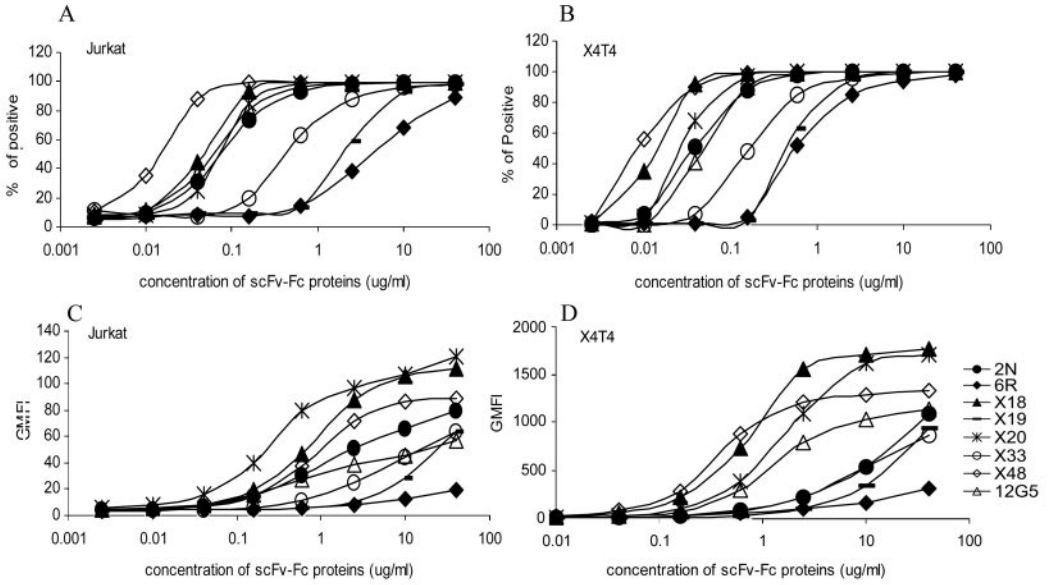

E

			X48	X18	X20	2N	X33	X19	6R	12G5
Jurkat	EC50 (μg/ml)	% positive	0.03±0.01	0.06±0.01	0.08±0.02	0.48±0.12	0.75±0.30	2.90±1.10	4.60±0.71	0.07±0.01
		By GMFI	0.10±0.01	1.80±0.28	1.00±0.48	2.50±0.19	5.90±0.14	15.20±1.40	7.80±0.75	0.91±0.19
	Relative $GMFI_{MAX}$		153.5±31.4	202.0±7.8	210.6±21.8	115.1±35.9	83.5±41.8	116.8±7.1	25.2±11.4	100
X4T4	EC50 (μg/ml)	% positive	0.02±0.01	0.01±0.006	0.03±0.00	0.12±0.04	0.18±0.02	0.63±0.13	1.90±0.49	0.05±0.01
		By GMFI	0.48±0.01	0.94±0.03	1.50±0.47	10.10±0.40	7.60±0.16	16.20±0.18	22.00±5.8	1.20±0.66
	Relative $GMFI_{MAX}$		127.9±11.7	160.6±6.3	164.5±20.3	82.8±18.9	81.5±7.3	90.3±9.9	25.5±3.1	100

FIGURE 3. Flow cytometric analysis of the anti-CXCR4 scFvFc Ab binding. Anti-CXCR4 scFvFc proteins or mAb 12G5 at the concentrations indicated on the X-axis were incubated with Jurkat (*A* and *C*) and X4T4 (*B* and *D*) cells followed by staining with FITC-conjugated goat anti-human IgG for scFvFc fusion proteins or FITC-conjugated goat anti-mouse IgG for 12G5. Cells stained with secondary Ab only were used as negative controls. Flow cytometric analysis was performed and binding activity of each Ab is presented as both percentage of positive cells (*A* and *B*) and absolute GMFI (*C* and *D*). *E*, A summary of the calculated EC_{50} and relative $GMFI_{MAX}$ (normalized by setting the absolute maximal GMFI of 12G5 as 100) of each anti-CXCR4 scFvFc Ab as mean ± SD from two experiments.

CXCR4 was replaced by CXCR2 (4442), only 7.5 and 18.2% binding activity was seen for 6R and X19, respectively, indicating that 6R and X19 are multidomain (MD) Abs and recognize both the Nt and ECL3 domains. In addition, because 6R was isolated by panning against the ΔN2–25-CXCR4 deletion mutant, its Nt epitope must be contained within the membrane proximal region of E26 to K38. The fact that X18 recognized the 2442 chimeras indicates that X18 is another MD Ab whose epitope contains ECL1 and/or ECL2 as well as Nt and ECL3.

To evaluate the effect of glycosylation at N11 of CXCR4, flow cytometric analysis of anti-CXCR4 scFvFc binding to stable Cf2-expressing CXCR4 wild type and N11Q mutant (20) were conducted. Although no effect on mAb12G5 binding was observed, as shown in Table III, the binding of Nt-directed 2N and X33 was

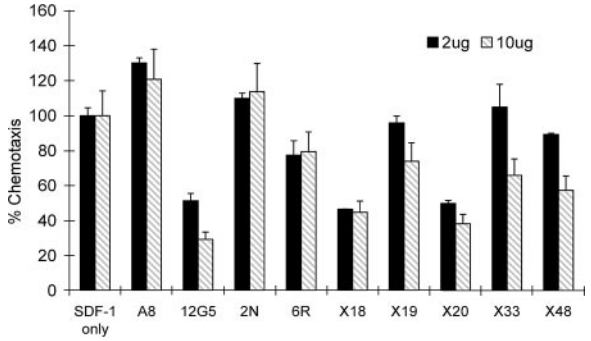

FIGURE 4. Inhibition of SDF-1α-induced chemotaxis on Jurkat cells by the anti-CXCR4 scFvFc Abs. The ability of the anti-CXCR4 scFvFc Abs to block SDF-1α-induced chemotaxis was assessed using the Transwell cell migration system in combination with flow cytometric counting of cells migrated to the bottom chamber containing SDF-1α at 50 ng/ml. Two and 10 μg of each Ab were tested. 12G5 IgG- and CCR5-specific A8scFvFc Abs were used as positive and negative control, respectively. Chemotaxis value in the absence of any Abs was set as 100%.

Table III. *Epitope mapping of CXCR4-specific Abs*[a]

	2N	6R	X18	X19	X20	X33	X48	12G5
Wt 4444	100	100	100	100	100	100	100	100
Wt 2222	4.7	−0.3	2	7.5	4.1	−0.5	−0.2	1.5
2444	2.3	8.7	32.2	9.1	8.0	2.5	5.4	83.5
2444b	5.3	8.7	34.5	15.8	9.0	3.4	6.8	98.5
4442	71.2	7.5	49.1	18.2	60.2	60.2	72.3	82.4
2442	5.6	9.0	47.9	12.8	8.5	6.1	7.1	102.6
N11Q	1.1	75.2	76.2	77.7	69.6	0.9	49.4	100.0

[a] Epitope mapping of anti-CXCR4 scFvFcs was determined with chimeric receptors composed of CXCR4 and CXCR2 and N11Q CXCR4 mutant. 2444 and 2444b indicate the first 27 or 38 N terminus amino acids of CXCR4 were replaced by CXCR2, respectively. 2442 means both NT (1–27) and ECL-3 were replaced by CXCR2 and wild-type CXCR2 is indicated as Wt 2222. 293T cells transiently transfected with CXCR4/CXCR2 chimeras or Cf2 cells stably expressing wild-type or N11Q mutant CXCR4 were stained with anti-CXCR4 scFvFc fusion proteins, followed by incubation with FITC-goat anti-human IgG. The binding activity was measured by GMFI on total cells gated. The reactivity to each clone = (GMFI of chimeric receptor/GMFI of wild-type CXCR4 on 293T) × 100% or = (GMFI of N11Q/GMFI of wild-type CXCR4 on Cf2) ×100%. The binding activities to wtCXCR4 of each clone were normalized as 100%.

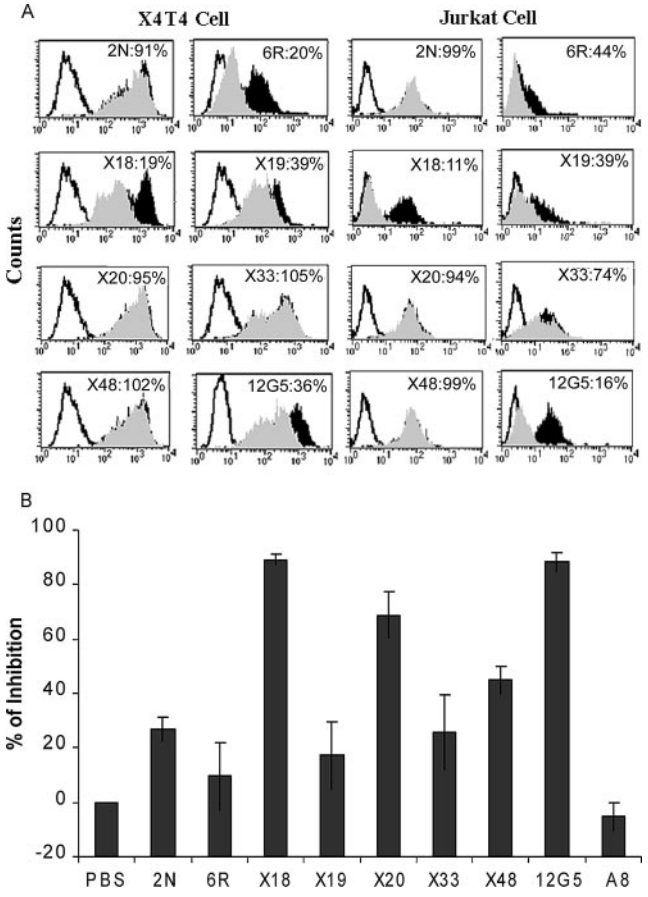

FIGURE 5. AMD3100 inhibition and 12G5 competition. *A*, Effect of AMD3100 on binding of anti-CXCR4 scFvFc Abs to X4T4 (*left*) or Jurkat (*right*) cells. The numbers in each histogram represents the relative binding intensity of the indicated Ab to cells pretreated with (gray fill) or without (black fill) AMD3100 as well as a FITC-labeled secondary Ab control (black line). *B*, 12G5 binding competition studies. X4T4 cells were preincubated with or without indicated Abs followed by staining with PE-conjugated 12G5. The value on the *y*-axis represents the percentage of 12G5 binding inhibition induced by pretreatment of cells with each Ab. The figure shows the mean ± SD from two experiments.

totally inhibited by the N11Q mutation. Thus, the N11 glycosylation site is essential for the Nt epitopes of 2N and X33. Inhibitions were ~50% for X48 and 22~30% for the other four clones, suggesting an important, although less critical, role for glycosylation at N11 in these Abs' epitope recognition.

AMD3100 inhibition and 12G5 competition studies. The interaction between the anti-CXCR4 scFvFcs and CXCR4 was further characterized in a binding competition assay with the small-molecule CXCR4 receptor antagonist AMD3100 through indirect immunofluorescence assay after preincubation of X4T4 or Jurkat cells with or without drug. As shown in Fig. 5*A*, treatment with AMD3100 had little to no effect on the binding activities of the Nt-directed Abs 2N, X20, X33, and X48 to X4T4 and Jurkat cells. For Abs that map to Nt/ECL3, inhibition of X19 binding to both cell lines was moderate (~60%) as was 6R binding to Jurkat cells (56%) while >80% inhibition of 6R binding to X4T4 cells was observed. Interestingly, AMD3100 markedly inhibited binding of the MD Ab X18 to X4T4 (81%) and Jurkat cells (89%). In addition, AMD3100 also inhibited mAb12G5 binding to X4T4 and Jurkat cells by 64 and 84%, respectively. These results are in agreement with data previously published by Carnec et al. (30) where a similar inhibition of MD mAb binding (anti-ECL2) but not anti-Nt mAb binding by AMD3100 was also observed.

Ab-competition studies were also performed by direct immunofluorescence assay using PE conjugated 12G5 mAb (Fig. 5*B*). No competition was seen with a control anti-CCR5 scFvFc Ab (A8), which does not bind CXCR4. In agreement with the chimeric mapping data, Nt-dependent 2N and X33 and Nt/ECL3 codependent 6R and X19 only weakly inhibited 12G5 binding. The MD Ab X18 that recognizes an epitope in ECL1/ECL2 was the strongest blocker (89%) of 12G5 binding. Surprisingly, X20 and X48 inhibited 12G5 binding by 69 and 45%, respectively, even though they both mapped to Nt suggesting that either 12G5 binding is not solely ECL2 dependent or that the inhibition may be caused more by steric hindrance than by direct epitope competition. The unlabeled 12G5 inhibited binding of its PE-conjugated form by ~88%.

Posttranslational tyrosine sulfation of a subset of anti-CXCR4 Abs and its effect on target Ag binding

Previous studies have demonstrated that sulfation of tyrosine residues in the V_H CDR3 occurs in a high percentage of human anti-HIV-1 gp120 CD4i mAbs which are directed against epitopes that overlap the CCR5 coreceptor binding sites. In about half the cases, tyrosine sulfation was functional and contributed to HIV-1 envelope recognition (31, 32). To date, such posttranslational modifications have not been reported in Abs that are directed to the chemokine coreceptors or to cellular proteins in general and therefore we sought to experimentally determine whether tyrosine sulfation of the anti-CXCR4 Abs could occur and whether such modification affects the Ab's binding affinity for CXCR4.

The sequence motif that specifies sulfation is only partially defined, with a dominant characteristic being three or four acidic residues within five residues of sulfotyrosine (32, 44). Instead of the known V_H CDR3 region, computational analysis using "Sulfinator" prediction software (32, 44, 45) identified residues at the V_L FW3-CDR3 boundary as potential sites for tyrosine sulfation (see Fig. 2, blue underline) for four of seven Abs (6R, X18, X33, and X48) (32, 44, 45). To determine whether posttranslational sulfation indeed occurred, 293T cells were transfected with Ab expression plasmids and were metabolically radiolabeled with either [^{35}S]cysteine/[^{35}S]methionine or [^{35}S]sulfate. The secreted Ab proteins in the culture supernatant were precipitated by protein A-Sepharose beads and analyzed by SDS-PAGE. As shown in Fig. 6*A*, all seven anti-CXCR4 scFvFc proteins were expressed and secreted into the culture supernatant albeit at different levels. Importantly, four of seven clones, 6R, X20, 2N, and X33, showed strong sulfation. It should be noted that only sulfation of 6R and X33 were originally predicted by the software. Human IgG1 Fc fragment fused with the wild-type N terminus of CCR5 and an N-terminal CCR5 mutant in which the four tyrosine residues were replaced by aspartic acid (DDDD) were used as sulfation positive and negative controls, respectively (23) (Q. Zhu, unpublished data).

Subsequent visual sequence inspection indicated that the V_H CDR2 and CDR3 (2N and X20) are two other regions that contained tyrosine residues flanked by acidic acid residues but did not achieve a high enough threshold to be predicted as tyrosine sulfation sites using the software. To further determine whether tyrosine residues were indeed the sites for sulfation, two of the four Abs X20 and X33 were chosen as examples and subjected to Y→D mutagenesis in V_H-CDR2 and V_L-FW3. As shown in Fig. 6*B*, although two of the mutations resulted in decreased total Ab expression (X20-$D^{59}D^{60}$ V_H-CDR2 and X33-$D^{86}D^{87}$ V_L-FW3), importantly, the $Y^{59}Y^{60}\rightarrow D^{59}D^{60}$ double mutation in V_H-CDR2 lead to undetectable sulfation in both Abs whereas only $Y^{86}\rightarrow D^{86}$ mutation in X20 V_L-FW3, but not $Y^{86}Y^{87}\rightarrow D^{86}D^{87}$ double mutation

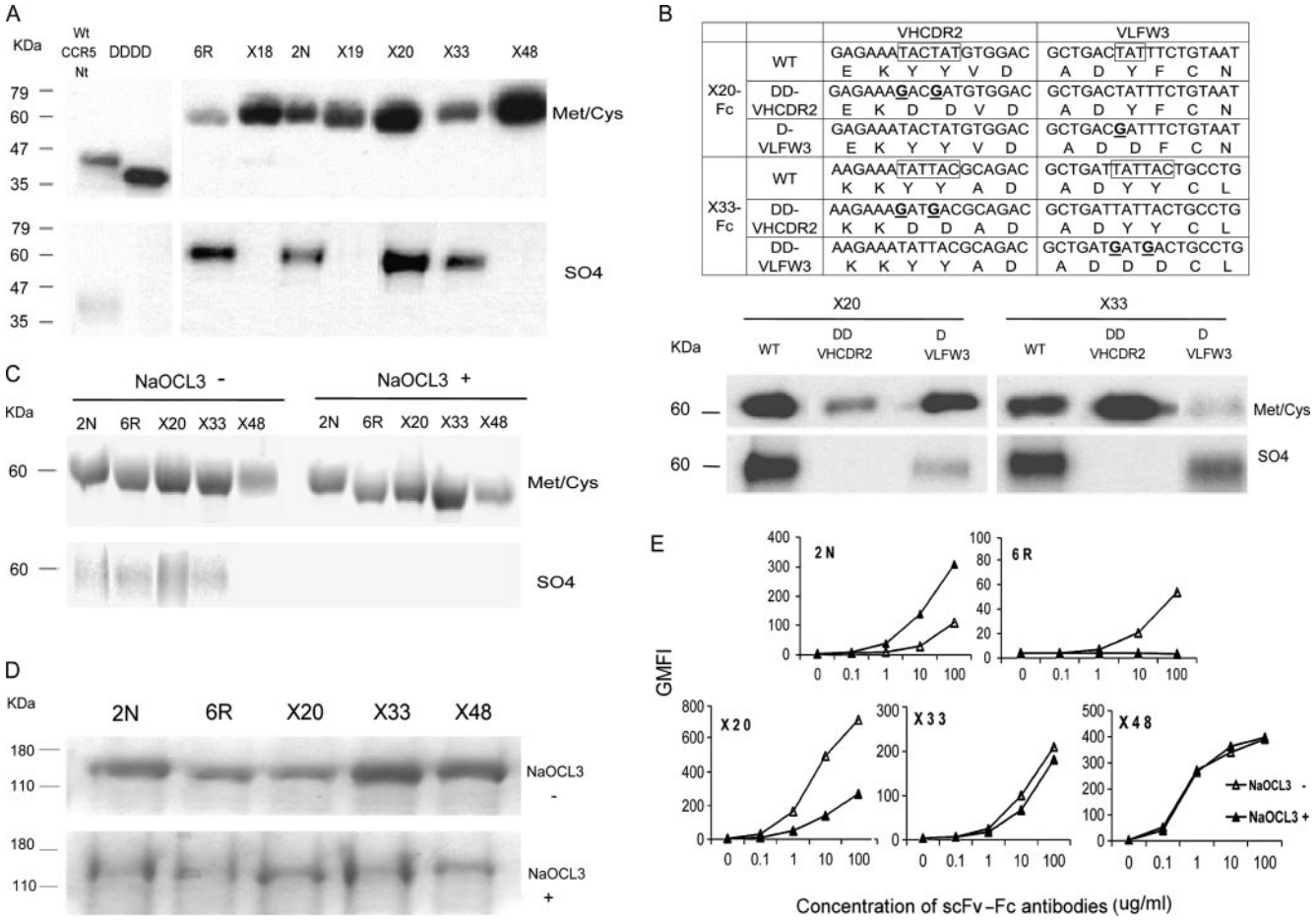

FIGURE 6. Studies on tyrosine sulfation of anti-CXCR4 scFvFc Abs. *A*, The [^{35}S]methionine/cysteine (*top*: Met/Cys) or [^{35}S]sulfate (bottom: SO_4) labeled Abs from transiently transfected 293T cell culture supernatants were immunoprecipitated, separated by SDS-PAGE analysis, and followed by autoradiography with wild-type and DDDD mutant CCR5 N-terminal-Fc fusion protein as positive and negative control, respectively. *B*, Tyrosine mutational analysis of X20 and X33 scFvFc Abs. The codons under investigation (*upper*) are boxed and the nucleotides mutated are in bold and underlined. The effect of tyrosine mutant on protein expression and sulfation were studied by radioimmunoprecipitation (*lower*) as described in *A*. *C–E*, Effect of sodium chlorate on the binding activity of anti-CXCR4 scFvFc Abs. *C*, [^{35}S]methionine/cysteine (*upper*: Met/Cys) or [^{35}S]sulfate (*lower*: SO_4) labeled Abs from transiently transfected 293T cell culture supernatants in the absence (*left*) or presence (*right*) of 100 mM sodium chlorate, were immunoprecipitated, separated by SDS-PAGE analysis under reducing conditions and followed by autoradiography. *D*, The anti-CXCR4 scFvFcs were purified from supernatant of 293T cells cultured in 293 SFM II serum-free medium in the absence (*upper*) or presence (*lower*) of 100 mM sodium chlorate, analyzed by SDS-PAGE under nonreducing conditions, and visualized by Coomassie Blue staining. *E*, Flow cytometric analysis of 5×10^5 X4T4 cells incubated with increased concentrations of the anti-CXCR4 scFvFcs purified as described in *D* above. Clone X48 Ab, which does not show sulfation modification, was used as a control. FITC-conjugated goat-anti-human IgG was used to detect the scFvFcs bound to the cell surface.

in X33 V_L FW3, had a small effect on sulfation. Due to the lower expression of the X20-$D^{59}D^{60}$ V_H-CDR2 mutant it is possible that sulfation at $Y^{86}Y^{87}$ of X20 V_L-FW3 was below detection limits. Thus, the results indicate that tyrosine sulfation occurred within V_H CDR2 for X20 and X33 scFvFc, and was also possible in V_L-FW3 for X20.

To further assess the functional role of tyrosine sulfation on the binding activity of anti-CXCR4 scFvFc Abs, 293T cells were transiently transfected with plasmids encoding the four sulfated and one nonsulfated X48 scFvFc. At 18 h posttransfection, the cells were washed and incubated in medium without or with 100 mM sodium chlorate, a relatively nontoxic inhibitor of sulfation (23, 46), for an additional 48 h. The culture supernatants containing secreted Ab were then collected, precipitated, and analyzed by SDS-PAGE. All of the scFvFcs were expressed, albeit at a lower level, in medium containing sodium chlorate (Fig. 6*D*) and sulfation was inhibited as determined by ^{35}S-sulfate labeling (Fig. 6*C*). Importantly, when their binding activities were examined on X4T4 cells, two of the four sulfated Abs (6R and X20) had markedly decreased binding activity while one Ab 2N showed an increase in its binding activity. No effect on binding was observed for the sulfated X33 or the control nonsulfated X48 Ab (Fig. 6*E*). Thus, tyrosine sulfation was functional in three of the four anti-CXCR4 Abs. The effects of tyrosine sulfation on binding activity were bidirectional and dependent on the individual Ab.

Discussion

In this study, PMPLs that incorporate purified human CXCR4 in its native conformation were used to screen a large human scFv Ab phage display library. Remarkably, despite the relatively low frequency of positive clones (~3%), a structurally and biochemically diverse panel of seven anti-CXCR4 Abs was isolated early in the selection process, from the second round of panning. This finding confirms and extends our previous report on the use of PMPLs to isolate human anti-CCR5 Abs (35). Thus, PMPLs containing purified seven transmembrane chemokine receptors provide a useful platform for the isolation of these human self-reactive Abs and appears to have clear advantages over other methods that rely on

Table IV. *Mapping and functional properties of human anti-CXCR4 scFv-Fcs*

Ab	V_H CDR3 Length[a]	V_H Replacement	Tyrosine Sulfation/Function[b]	CXCR2/CXCR4[c]	Nt Glycosylation Dependency[d]	AMD3100 Inhibition[e]	12G5 Competition[f]	SDF1α Chemotaxis Inhibition[g]
2N	S	−	Y/↓	Nt	++++	−	+	−
6R	S	+	Y/↑	Nt_{26-38} ECL3	+	++ J → +++ Cf2	−	+
X18	L	−	$N/_{N/A}$	Nt ECL1/2/3	+	++++	++++	+++
X19	S	+	$N/_{N/A}$	Nt ECL3	+	+++	−	+
X20	L	−	Y/↑	Nt	+	−	+++	+++
X33	L	−	Y/−	Nt	++++	− Cf2 → + J	+	+
X48	S	−	$N/_{N/A}$	Nt	++	−	++	++
12G5	N/A	N/A	N/A	ECL1/2	−	+++ Cf2 → ++++ J	++++	++++

[a] S, Short, 8∼13 aa; L, long, 17∼18 aa.
[b] Y, Sulfation; N, no sulfation; ↑, sulfation improves binding activity; ↓, sulfation reduces binding activity; N/A, not applicable.
[c] Epitope is defined as the following: when the binding of an scFvFc is reduced >75%, the CXCR4 domain replaced by that of CXCR2 is considered the major epitope(s) for the Ab tested.
[d] N11 glycosylation dependency and [e] AMD3100 inhibition on Ab binding: effects are defined as N11Q vs. wtCXCR4 Cf2 cells or AMD3100 + vs. − Jurkat and X4T4 cells as reflected by percentage of GMFI: "++++": <20%; "+++": 20∼40%; "++": 40∼60%; "+": 60∼80%; "-": >80%.
[f] Percentage of 12G5-binding inhibition: "−": <20%; "+": 20∼40%; "++": 40∼60%; "+++": 60∼80%; "++++": >80%.
[g] Percentage of chemotaxis inhibition: "−": <10%; "+": 10∼30%; "++": 30∼50%; "+++": 50∼70%; "++++": >70%.

natural ligands or preexisting Abs (47–49) or use isolated fragments of the receptor in the Ab discovery process (50).

V_H replacement has recently been shown to contribute to the primary B cell repertoire in humans (41, 51). In addition to extending the length of the CDR3 region, V_H replacement footprints have been shown to preferentially contribute charged amino acids. In immature B cells, V_H replacement may also contribute to the generation of Abs reactive to self Ags (39, 52, 53). Moreover, the higher frequency of V_H replacement products has been reported in different autoimmune diseases and in the H chain of IgG genes encoding autoantibodies, ~21–30% (54), comparing with a ~5% V_H replacement frequency in normal IgGs, respectively. In the present study, genetic analysis provided evidence that V_H replacement has contributed to V_H CDR3 diversity for two of the seven CXCR4 Abs (29%). However, neither of these Abs had long V_H CDR3 regions and only one charged amino acid (His) was introduced into Ab 6R through V_H replacement. Nevertheless, these observations provide additional evidence that V_H replacement does contribute to the repertoire of V_H genes with specific binding activity for CXCR4 and support the hypothesis that V_H gene replacement contributes to autoantibody formation and plays a potential role in autoimmunity.

It has been proposed that the tyrosine sulfation of V_H CDR3 residues represents a unique property of anti-HIV-1 gp120 CD4i Abs that evolved to enhance viral Ag recognition by molecular mimicry of the coreceptor which also contains sulfated tyrosines in its N-terminal domain (31, 32). In this report, biochemical analysis demonstrated that sulfation occurred in four of the seven anti-CXCR4 Abs examined. Importantly, sulfation contributed to the function of three of these Abs with bidirectional effects of increase or decrease in binding affinity for CXCR4. Mutagenesis studies further demonstrated that tyrosine sulfation occurred in V_H CDR2 and possibly V_L-FW3, areas where tyrosine sulfation had not been previously described (31, 32). These results demonstrate that tyrosine sulfation can directly contribute to the binding activity of Abs that recognize self-Ags. The possible role that tyrosine-sulfated proteins may play in the pathogenesis of autoimmune disease has recently been reviewed (33) and should now be extended, based on this report, to include tyrosine-sulfated autoreactive Abs. The results also suggest that tyrosine sulfation may contribute in a much greater way than previously recognized to the binding activity of Abs that are expressed in mammalian cells and may, in part, be responsible for the often seen increase in binding affinity which has been attributed to the effect of bivalency on Ab avidity when converting monovalent scFvs expressed by phage display into whole human IgGs. Furthermore, because the predictive software for tyrosine sulfation performed poorly in our studies, it is likely that the involvement of tyrosine sulfation on Ab binding will need to be determined on a case-by-case basis until a better understanding of tyrosine sulfation of Ab V regions is obtained and sufficient data is collected.

Two previous studies that examined 12G5 and a panel of seven murine anti-CXCR4 mAbs provided the initial evidence of antigenically distinct conformations of CXCR4. Most of these Abs were mapped to ECL2 and their binding affinities varied within a 2.5-fold range (29, 30). Baribaud et al. (29) demonstrated that CXCR4 is expressed in at least two different conformations on the cell surface that was variable among the different primary cells and cell lines tested. Carnec et al. (30) reported the existence of multiple CXCR4 subpopulations that did not vary in a cell-specific manner. Both groups proposed that the mAbs with highest maximal binding could recognize the widest range of CXCR4 conformations. In the present studies, the panel of anti-CXCR4 scFvFcs demonstrated different binding affinities and levels of maximal binding that were not cell type specific. Indeed, the rank order of maximal scFvFc binding was essentially identical for Jurkat and X4T4 cells. These results suggest that each of these cell lines not only displayed antigenic heterogeneity but also a fixed mixture of different antigenic conformers of CXCR4 (Fig. 3). For example, 12G5, a commonly used conformation-dependent mAb, can only bind to a subpopulation of CXCR4 molecules on the cell surface. The maximal binding of X18 and X20 is much higher than those of X48 and 12G5 suggesting that these Abs recognize more widely expressed or accessible epitopes. The molecular basis of this antigenic heterogeneity is unknown but may involve variability in posttranslational modifications of CXCR4 including *N*-glycosylation (18–20), tyrosine (22, 23) and serine chondroitin sulfation (22), and N-terminal processing (26–28). CXCR4 structure may also vary as a result of conformational fluctuations, receptor oligomerization, neighbor protein associations, and G-protein coupling (30, 55). The relationship between conformational heterogeneity of CXCR4 and certain disease states requires further exploration.

Epitope mapping studies of the Abs using CXCR2/CXCR4 chimeras, binding to N11Q CXCR4 mutant receptor proteins, AMD3100 inhibition and 12G5 competition, demonstrated the complex nature of the epitopes exposed on the surface of this seven transmembrane spanning receptor. Table IV summarizes these findings. The fact that all seven Abs recognized the Nt domain to a variable extent may be related to the enhanced exposure

of this region in the CXCR4-PMPLs. Complete loss of 2N and X33 binding to the CXCR4 N11Q glycosylation site mutant demonstrated the critical role of this region in epitope recognition. It should be noted that several Abs exhibited properties of multidomain Abs and each had a unique profile. It was observed that the Abs most dependent on the Nt domain for binding were the least inhibitable by AMD3100, which is in agreement with previous reports that the binding sites for this small molecular bicyclam CXCR4 antagonist are negatively charged aspartates located at amino acid 171 (transmembrane domain (TM) 4), 262 (TM6) as well as 182 (ECL2) and 193 (ECL2) of CXCR4 (56, 57). The moderate inhibition of 6R and X19 binding is likely due to the recognition by both Abs and AMD3100 of Asp262 at the TM6/ECL3 boundary. In addition, it has been suggested that an alteration in conformation of CXCR4 occurs following AMD3100 binding. Because AMD3100 also reacts with two aspartic acid residues in ECL2 and X18 maps to this region, the strong AMD3100 inhibition of X18 binding may be secondary to an overlap between the X18 epitope with the binding site of AMD3100 or the antagonist-induced changes in the structure of CXCR4 that effects the X18 overlap.

Structural and mutagenesis studies have demonstrated that the N-terminal domain of CXCR4 plays an important role in SDF-1α binding while residues in the ECL2 are important for signaling (37, 58, 59). To investigate this relationship in more depth, Ab-mediated inhibition of SDF-1α chemotaxis was examined to identify important structure-function relationships between the epitope recognized and signaling inhibited by the different Abs. Several important observations were made. First, although six of seven Abs inhibited SDF-1α chemotaxis, the inhibition was not uniform. The Abs X18, X20, as well as X48, showed superior inhibition of chemotaxis and there was a strong correlation between inhibition and the amount of Ab that bound to Jurkat cells. Another commonality is that these Abs also recognize an epitope that overlaps with 12G5. Interestingly, 12G5 was a potent chemotaxis inhibitor despite a lower $GMFI_{MAX}$ binding, suggesting that its epitope overlaps with a site critical for SDF-1α signaling presumably located in the ECL2 domain. The Abs that bound to Nt alone (X33) or to Nt and ECL3 (6R, X19) were the weakest inhibitors of chemotaxis and also have the lowest levels of saturable binding. Ab 2N, which is purely Nt binding (Table III), showed no inhibition of chemotaxis. These results confirm previous reports that while Nt is important in SDF-1α binding, there is greater dependence of the extracellular domains of CXCR4, in particular ECL2, in SDF-1α signaling.

In summary, CXCR4 exists in multiple antigenic states on the cell surface and a panel of human Abs has been identified to further probe CXCR4 expression and function. All of the Abs recognize the Nt to variable extents and several Abs bind to multiple domains. Thus, these Abs provide important new tools to examine the biology of CXCR4 in greater detail such as the extent to which posttranslational modifications and Nt-proteolytic cleavage of CXCR4 affect antigenic structure (26, 27) as well as the biological activity of the CXCR4-SDF-1 axis in health and disease. In addition, the Abs can be useful in several areas of investigation in which a central involvement of the CXCR4/SDF-1 axis has been established such as in the bone marrow niche for the homing and egress of adult stem cells (60). The expression of CXCR4 isoforms by different cancer cells and cancer stem cells and their importance for cancer cell survival and metastases can now be explored (14, 61) as can the differential expression and effects of these CXCR4 isoforms in neoangiogenesis (62, 63). Although selective modulation of this axis in vivo has tremendous therapeutic potential, the diverse involvement of CXCR4 in so many biological processes will challenge this potential because some level of steady-state homeostasis of CXCR4/SDF-1 is needed for response to physiologic stress or damage as part of the normal host defense and repair mechanism (64). The antigenic complexity of the known intracellular stores of CXCR4 (65) will also need to be considered as will the involvement of CXCR4-expressing cellular microparticles (66, 67) because their mobilization and transfer to the cell surface, respectively, can also lead to new and variable SDF-1 biological responses. Although the challenges of modulating this axis in vivo are formidable, the translational potential is even more compelling. Human mAb immunotherapy may be one way to approach this problem because it has the advantage of targeting defined CXCR4 antigenic structures that can provide some degree of selectivity in vivo.

Acknowledgments

We thank Dr. Dana Gabuzda for providing the stable N11Q-CXCR4 stable Cf2D4 cell line.

Disclosures

The authors have no financial conflict of interest.

References

1. Juarez, J., L. Bendall, and K. Bradstock. 2004. Chemokines and their receptors as therapeutic targets: the role of the SDF-1/CXCR4 axis. *Curr. Pharm. Des.* 10: 1245–1259.
2. Knaut, H., C. Werz, R. Geisler, and C. Nusslein-Volhard. 2003. A zebrafish homologue of the chemokine receptor Cxcr4 is a germ-cell guidance receptor. *Nature* 421: 279–282.
3. Murdoch, C. 2000. CXCR4: chemokine receptor extraordinaire. *Immunol. Rev.* 177: 175–184.
4. Rossi, D., and A. Zlotnik. 2000. The biology of chemokines and their receptors. *Annu. Rev. Immunol.* 18: 217–242.
5. Sallusto, F., C. R. Mackay, and A. Lanzavecchia. 2000. The role of chemokine receptors in primary, effector, and memory immune responses. *Annu. Rev. Immunol.* 18: 593–620.
6. Muller, A., B. Homey, H. Soto, N. Ge, D. Catron, M. E. Buchanan, T. McClanahan, E. Murphy, W. Yuan, S. N. Wagner, et al. 2001. Involvement of chemokine receptors in breast cancer metastasis. *Nature* 410: 50–56.
7. Murakami, T., W. Maki, A. R. Cardones, H. Fang, A. Tun Kyi, F. O. Nestle, and S. T. Hwang. 2002. Expression of CXC chemokine receptor-4 enhances the pulmonary metastatic potential of murine B16 melanoma cells. *Cancer Res.* 62: 7328–7334.
8. Zeelenberg, I. S., L. Ruuls-Van Stalle, and E. Roos. 2003. The chemokine receptor CXCR4 is required for outgrowth of colon carcinoma micrometastases. *Cancer Res.* 63: 3833–3839.
9. Burger, J. A., and T. J. Kipps. 2006. CXCR4: a key receptor in the crosstalk between tumor cells and their microenvironment. *Blood.* 107: 1761–1767.
10. Kakinuma, T., and S. T. Hwang. 2006. Chemokines, chemokine receptors, and cancer metastasis. *J. Leukocyte Biol.* 79: 639–651.
11. Balkwill, F. 2004. Cancer and the chemokine network. *Nat. Rev. Cancer* 4: 540–550.
12. Balkwill, F. 2004. The significance of cancer cell expression of the chemokine receptor CXCR4. *Semin. Cancer Biol.* 14: 171–179.
13. Zlotnik, A. 2004. Chemokines in neoplastic progression. *Semin. Cancer Biol.* 14: 181–185.
14. Ratajczak, M. Z., E. Zuba-Surma, M. Kucia, R. Reca, W. Wojakowski, and J. Ratajczak. 2006. The pleiotropic effects of the SDF-1-CXCR4 axis in organogenesis, regeneration and tumorigenesis. *Leukemia* 20: 1915–1924.
15. Berger, E. A., P. M. Murphy, and J. M. Farber. 1999. Chemokine receptors as HIV-1 coreceptors: roles in viral entry, tropism, and disease. *Annu. Rev. Immunol.* 17: 657–700.
16. Doms, R. W. 2001. Chemokine receptors and HIV entry. *AIDS* 15(Suppl. 1): S34–S35.
17. Kryczek, I., S. Wei, E. Keller, R. Liu, and W. Zou. 2006. Stromal derived factor (SDF-1/CXCL12) and human tumor pathogenesis. *Am. J. Physiol.* 292: C987–C995.
18. Chabot, D. J., H. Chen, D. S. Dimitrov, and C. C. Broder. 2000. *N*-linked glycosylation of CXCR4 masks coreceptor function for CCR5-dependent human immunodeficiency virus type 1 isolates. *J. Virol.* 74: 4404–4413.
19. Sloane, A. J., V. Raso, D. S. Dimitrov, X. Xiao, S. Deo, N. Muljadi, D. Restuccia, S. Turville, C. Kearney, C. C. Broder, et al. 2005. Marked structural and functional heterogeneity in CXCR4: separation of HIV-1 and SDF-1α responses. *Immunol Cell. Biol.* 83: 129–143.
20. Wang, J., G. J. Babcock, H. Choe, M. Farzan, J. Sodroski, and D. Gabuzda. 2004. *N*-linked glycosylation in the CXCR4 N-terminus inhibits binding to HIV-1 envelope glycoproteins. *Virology* 324: 140–150.
21. Chabot, D. J., P. F. Zhang, G. V. Quinnan, and C. C. Broder. 1999. Mutagenesis of CXCR4 identifies important domains for human immunodeficiency virus type

1 X4 isolate envelope-mediated membrane fusion and virus entry and reveals cryptic coreceptor activity for R5 isolates. *J. Virol.* 73: 6598–6609.
22. Farzan, M., G. J. Babcock, N. Vasilieva, P. L. Wright, E. Kiprilov, T. Mirzabekov, and H. Choe. 2002. The role of post-translational modifications of the CXCR4 amino terminus in stromal-derived factor 1 α association and HIV-1 entry. *J. Biol. Chem.* 277: 29484–29489.
23. Farzan, M., T. Mirzabekov, P. Kolchinsky, R. Wyatt, M. Cayabyab, N. P. Gerard, C. Gerard, J. Sodroski, and H. Choe. 1999. Tyrosine sulfation of the amino terminus of CCR5 facilitates HIV-1 entry. *Cell* 96: 667–676.
24. Lapham, C. K., M. B. Zaitseva, S. Lee, T. Romanstseva, and H. Golding. 1999. Fusion of monocytes and macrophages with HIV-1 correlates with biochemical properties of CXCR4 and CCR5. *Nat. Med.* 5: 303–308.
25. Wang, J., L. He, C. A. Combs, G. Roderiquez, and M. A. Norcross. 2006. Dimerization of CXCR4 in living malignant cells: control of cell migration by a synthetic peptide that reduces homologous CXCR4 interactions. *Mol. Cancer Ther.* 5: 2474–2483.
26. Valenzuela-Fernandez, A., T. Planchenault, F. Baleux, I. Staropoli, K. Le-Barillec, D. Leduc, T. Delaunay, F. Lazarini, J. L. Virelizier, M. Chignard, et al. 2002. Leukocyte elastase negatively regulates stromal cell-derived factor-1 (SDF-1)/CXCR4 binding and functions by amino-terminal processing of SDF-1 and CXCR4. *J. Biol. Chem.* 277: 15677–15689.
27. Levesque, J. P., J. Hendy, Y. Takamatsu, P. J. Simmons, and L. J. Bendall. 2003. Disruption of the CXCR4/CXCL12 chemotactic interaction during hematopoietic stem cell mobilization induced by GCSF or cyclophosphamide. *J. Clin. Invest.* 111: 187–196.
28. Lapidot, T., and I. Petit. 2002. Current understanding of stem cell mobilization: the roles of chemokines, proteolytic enzymes, adhesion molecules, cytokines, and stromal cells. *Exp. Hematol.* 30: 973–981.
29. Baribaud, F., T. G. Edwards, M. Sharron, A. Brelot, N. Heveker, K. Price, F. Mortari, M. Alizon, M. Tsang, and R. W. Doms. 2001. Antigenically distinct conformations of CXCR4. *J. Virol.* 75: 8957–8967.
30. Carnec, X., L. Quan, W. C. Olson, U. Hazan, and T. Dragic. 2005. Anti-CXCR4 monoclonal antibodies recognizing overlapping epitopes differ significantly in their ability to inhibit entry of human immunodeficiency virus type 1. *J. Virol.* 79: 1930–1933.
31. Choe, H., W. Li, P. L. Wright, N. Vasilieva, M. Venturi, C. C. Huang, C. Grundner, T. Dorfman, M. B. Zwick, L. Wang, et al. 2003. Tyrosine sulfation of human antibodies contributes to recognition of the CCR5 binding region of HIV-1 gp120. *Cell* 114: 161–170.
32. Huang, C. C., M. Venturi, S. Majeed, M. J. Moore, S. Phogat, M. Y. Zhang, D. S. Dimitrov, W. A. Hendrickson, J. Robinson, J. Sodroski, et al. 2004. Structural basis of tyrosine sulfation and V_H-gene usage in antibodies that recognize the HIV type 1 coreceptor-binding site on gp120. *Proc. Natl. Acad. Sci. USA* 101: 2706–2711.
33. Hsu, W., G. L. Rosenquist, A. A. Ansari, and M. E. Gershwin. 2005. Autoimmunity and tyrosine sulfation. *Autoimmun. Rev.* 4: 429–435.
34. Babcock, G. J., T. Mirzabekov, W. Wojtowicz, and J. Sodroski. 2001. Ligand binding characteristics of CXCR4 incorporated into paramagnetic proteoliposomes. *J. Biol. Chem.* 276: 38433–38440.
35. Mirzabekov, T., H. Kontos, M. Farzan, W. Marasco, and J. Sodroski. 2000. Paramagnetic proteoliposomes containing a pure, native, and oriented seven-transmembrane segment protein, CCR5. *Nat. Biotechnol.* 18: 649–654.
36. Bai, J., J. Sui, R. Y. Zhu, A. S. Tallarico, F. Gennari, D. Zhang, and W. A. Marasco. 2003. Inhibition of Tat-mediated transactivation and HIV-1 replication by human anti-hCyclinT1 intrabodies. *J. Biol. Chem.* 278: 1433–1442.
37. Doranz, B. J., M. J. Orsini, J. D. Turner, T. L. Hoffman, J. F. Berson, J. A. Hoxie, S. C. Peiper, L. F. Brass, and R. W. Doms. 1999. Identification of CXCR4 domains that support coreceptor and chemokine receptor functions. *J. Virol.* 73: 2752–2761.
38. Reth, M., P. Gehrmann, E. Petrac, and P. Wiese. 1986. A novel V_H to V_HDJ_H joining mechanism in heavy-chain-negative (null) pre-B cells results in heavy-chain production. *Nature* 322: 840–842.
39. Radic, M. Z., and M. Zouali. 1996. Receptor editing, immune diversification, and self-tolerance. *Immunity* 5: 505–511.
40. Nemazee, D., and M. Weigert. 2000. Revising B cell receptors. *J. Exp. Med.* 191: 1813–1817.
41. Zhang, Z., M. Zemlin, Y. H. Wang, D. Munfus, L. E. Huye, H. W. Findley, S. L. Bridges, D. B. Roth, P. D. Burrows, and M. D. Cooper. 2003. Contribution of V_h gene replacement to the primary B cell repertoire. *Immunity* 19: 21–31.
42. Lu, Z., J. F. Berson, Y. Chen, J. D. Turner, T. Zhang, M. Sharron, M. H. Jenks, Z. Wang, J. Kim, J. Rucker, et al. 1997. Evolution of HIV-1 coreceptor usage through interactions with distinct CCR5 and CXCR4 domains. *Proc. Natl. Acad. Sci. USA* 94: 6426–6431.
43. Brelot, A., N. Heveker, K. Adema, M. J. Hosie, B. Willett, and M. Alizon. 1999. Effect of mutations in the second extracellular loop of CXCR4 on its utilization by human and feline immunodeficiency viruses. *J. Virol.* 73: 2576–2586.
44. Moore, K. L. 2003. The biology and enzymology of protein tyrosine *O*-sulfation. *J. Biol. Chem.* 278: 24243–24246.
45. Monigatti, F., E. Gasteiger, A. Bairoch, and E. Jung. 2002. The Sulfinator: predicting tyrosine sulfation sites in protein sequences. *Bioinformatics* 18: 769–770.
46. Mintz, K. P., L. W. Fisher, W. J. Grzesik, V. C. Hascall, and R. J. Midura. 1994. Chlorate-induced inhibition of tyrosine sulfation on bone sialoprotein synthesized by a rat osteoblast-like cell line (UMR 106-01 BSP). *J. Biol. Chem.* 269: 4845–4852.
47. Osbourn, J. K., E. J. Derbyshire, T. J. Vaughan, A. W. Field, and K. S. Johnson. 1998. Pathfinder selection: in situ isolation of novel antibodies. *Immunotechnology* 3: 293–302.
48. Osbourn, J. K., J. C. Earnshaw, K. S. Johnson, M. Parmentier, V. Timmermans, and J. McCafferty. 1998. Directed selection of MIP-1α neutralizing CCR5 antibodies from a phage display human antibody library. *Nat. Biotechnol.* 16: 778–781.
49. Sui, J., J. Bai, A. St Clair Tallarico, C. Xu, and W. A. Marasco. 2003. Identification of CD4 and transferrin receptor antibodies by CXCR4 antibody-guided Pathfinder selection. *Eur. J. Biochem.* 270: 4497–4506.
50. Vaday, G. G., S. B. Hua, D. M. Peehl, M. H. Pauling, Y. H. Lin, L. Zhu, D. M. Lawrence, H. D. Foda, and S. Zucker. 2004. CXCR4 and CXCL12 (SDF-1) in prostate cancer: inhibitory effects of human single chain Fv antibodies. *Clin. Cancer Res.* 10: 5630–5639.
51. Zhang, Z., P. D. Burrows, and M. D. Cooper. 2004. The molecular basis and biological significance of V_H replacement. *Immunol. Rev.* 197: 231–242.
52. Nussenzweig, M. C. 1998. Immune receptor editing: revise and select. *Cell* 95: 875–878.
53. King, L. B., and J. G. Monroe. 2001. Immunology: B cell receptor rehabilitation—pausing to reflect. *Science* 291: 1503–1505.
54. Liu, Y., R. Fan, S. Zhou, Z. Yu, and Z. Zhang. 2005. Potential contribution of V_H gene replacement in immunity and disease. *Ann. NY Acad. Sci.* 1062: 175–181.
55. Kenakin, T. 2004. Principles: receptor theory in pharmacology. *Trends Pharmacol. Sci.* 25: 186–192.
56. Hatse, S., K. Princen, L. O. Gerlach, G. Bridger, G. Henson, E. De Clercq, T. W. Schwartz, and D. Schols. 2001. Mutation of Asp^{171} and Asp^{262} of the chemokine receptor CXCR4 impairs its coreceptor function for human immunodeficiency virus-1 entry and abrogates the antagonistic activity of AMD3100. *Mol. Pharmacol.* 60: 164–173.
57. Gerlach, L. O., R. T. Skerlj, G. J. Bridger, and T. W. Schwartz. 2001. Molecular interactions of cyclam and bicyclam non-peptide antagonists with the CXCR4 chemokine receptor. *J. Biol. Chem.* 276: 14153–14160.
58. Brelot, A., N. Heveker, M. Montes, and M. Alizon. 2000. Identification of residues of CXCR4 critical for human immunodeficiency virus coreceptor and chemokine receptor activities. *J. Biol. Chem.* 275: 23736–23744.
59. Zhou, N., Z. Luo, J. Luo, D. Liu, J. W. Hall, R. J. Pomerantz, and Z. Huang. 2001. Structural and functional characterization of human CXCR4 as a chemokine receptor and HIV-1 co-receptor by mutagenesis and molecular modeling studies. *J. Biol. Chem.* 276: 42826–42833.
60. Lapidot, T., A. Dar, and O. Kollet. 2005. How do stem cells find their way home? *Blood* 106: 1901–1910.
61. Dar, A., O. Kollet, and T. Lapidot. 2006. Mutual, reciprocal SDF-1/CXCR4 interactions between hematopoietic and bone marrow stromal cells regulate human stem cell migration and development in NOD/SCID chimeric mice. *Exp. Hematol.* 34: 967–975.
62. Shepherd, R. M., B. J. Capoccia, S. M. Devine, J. Dipersio, K. M. Trinkaus, D. Ingram, and D. C. Link. 2006. Angiogenic cells can be rapidly mobilized and efficiently harvested from the blood following treatment with AMD3100. *Blood* 108: 3662–3667.
63. Jin, D. K., K. Shido, H. G. Kopp, I. Petit, S. V. Shmelkov, L. M. Young, A. T. Hooper, H. Amano, S. T. Avecilla, B. Heissig, et al. 2006. Cytokine-mediated deployment of SDF-1 induces revascularization through recruitment of $CXCR4^+$ hemangiocytes. *Nat. Med.* 12: 557–567.
64. Imai, K., M. Kobayashi, J. Wang, N. Shinobu, H. Yoshida, J. Hamada, M. Shindo, F. Higashino, J. Tanaka, M. Asaka, and M. Hosokawa. 1999. Selective secretion of chemoattractants for haemopoietic progenitor cells by bone marrow endothelial cells: a possible role in homing of haemopoietic progenitor cells to bone marrow. *Br. J. Haematol.* 106: 905–911.
65. Dar, A., P. Goichberg, V. Shinder, A. Kalinkovich, O. Kollet, N. Netzer, R. Margalit, M. Zsak, A. Nagler, I. Hardan, et al. 2005. Chemokine receptor CXCR4-dependent internalization and resecretion of functional chemokine SDF-1 by bone marrow endothelial and stromal cells. *Nat. Immunol.* 6: 1038–1046.
66. Kalinkovich, A., S. Tavor, A. Avigdor, J. Kahn, A. Brill, I. Petit, P. Goichberg, M. Tesio, N. Netzer, E. Naparstek, et al. 2006. Functional CXCR4-expressing microparticles and SDF-1 correlate with circulating acute myelogenous leukemia cells. *Cancer Res.* 66: 11013–11020.
67. Janowska-Wieczorek, A., M. Majka, J. Kijowski, M. Baj-Krzyworzeka, R. Reca, A. R. Turner, J. Ratajczak, S. G. Emerson, M. A. Kowalska, and M. Z. Ratajczak. 2001. Platelet-derived microparticles bind to hematopoietic stem/progenitor cells and enhance their engraftment. *Blood* 98: 3143–3149.